From Benzene to Muconaldehyde: Theoretical Mechanistic Investigation on Some Tropospheric Oxidation Channels

Giovanni Ghigo and Glauco Tonachini*

Contribution from the Dipartimento di Chimica Generale ed Organica Applicata, Università di Torino, Corso Massimo D'Azeglio 48, 10125 Torino, Italy

Received February 22, 1999. Revised Manuscript Received June 22, 1999

Abstract: In the tropospheric oxidation of benzene and methylated benzenes, unsaturated dicarbonyls are commonly detected products. Aldehydes are known to contribute on their own to some aspects of air pollution, and hexa-2,4-dien-1,6-dial (muconaldehyde) in particular is interesting because of its multiform toxicity. This study investigates the likelyhood of some benzene oxidation steps and is especially focused on ring opening and generation of muconaldehyde. With sufficiently *high NO_x concentration*, O abstraction by NO from the cis peroxyl group in the 2-hydroxy-cyclohexadienyl peroxyl radical **III** can play a role. In fact, it is shown to open a facile cascade of oxidation steps by first forming the 2-hydroxy-cyclohexadienyl oxyl radical **VI**. This intermediate is prone to ring opening via β-fragmentation and generates the open-chain delocalized 6-hydroxy-hexa-2,4-dienalyl radical **VII**, in which one terminus is the first carbonyl group of the final dialdehyde. The second one can form either by simple H abstraction operated by O_2 or by O_2 addition followed by $HOO^{\bullet}$ elimination. The overall free-energy drop with respect to **III** is estimated to be 48 kcal mol^{-1}. Exploration of other pathways, possibly playing a major role in yielding aldehydes in the case of *low NO_x concentration*, indicates that only ring closure of the 2-hydroxy-cyclohexadienyl peroxyl radical **III** to the [3.2.1] bicyclic endo-peroxy allyl radical intermediate **XIII** is promising. In this case, however, the outcome of a subsequent ring opening can ultimately be the production of 1,2 and 1,4 dialdehydes (as direct oxidation of muconaldehyde itself can actually do).

Introduction

In the tropospheric oxidation of hydrocarbons, aromatics (especially benzene and the methylated benzenes) are a very important component, particularly in polluted areas.[1−3] Unsaturated carbonyls and phenol are detected. The addition of $HO^{\bullet}$ to the aromatic ring, yielding a hydroxycyclohexadienyl radical (the so-called benzene-OH adduct, **I** in Scheme 1), is commonly considered to be the prevalent reaction in initiating benzene oxidation. Phenol formation can occur by simple H abstraction. Unsaturated carbonyls can form through several steps, which see the intervention of O_2, $HO^{\bullet}$, and nitrogen oxides (NO_x). The detailed mechanism of the degradation steps following the formation of **I** is still debated, though a considerable number of experimental studies has been carried out in the past years. The role of O_2 is intertwined with that of NO and NO_2, and their relative importance is mainly a function of the NO_x concentration. The hydroxycyclohexadienyl radical **I** initially formed has been found to react more rapidly with NO_2 than with NO, and even more slowly with O_2,[4] on the basis of the relevant rate constants. But this implies that, if their relative abundance in the troposphere is considered, the latter reaction is more important.[3] Actually, going through the extensive and diverse experimental literature leaves one with the impression that some important aspects of the evolution of aromatic pollutants in the atmosphere are still to be clearly described. To exemplify one of the difficulties which can be encountered, we can mention that experiments carried out with variable $[O_2]$/

Scheme 1

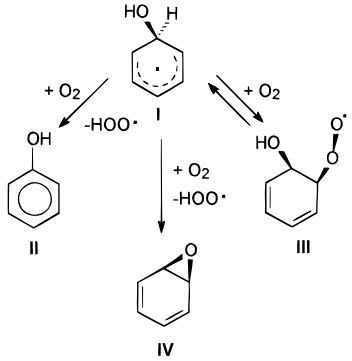

* Corresponding author. E-mail: tonachini@silver.ch.unito.it. Fax: 39-011-6707642.

(1) (a) Becker, K. H.; Barnes, I.; Ruppert, L.; Wiesen, P. Free Radicals in the Atmosphere: the Motor of Tropospheric Oxidation Processes. In *Free Radicals in Biology and Environment*; Minisci, F., Ed.; Kluwer Academic Publishers: The Netherlands, 1997; Chapter 27, pp 365−385, and references therein. (b) Güsten, H. Degradation of Atmospheric Pollutants by Tropospheric Free Radical Reactions. In *Free Radicals in Biology and Environment*; Minisci, F., Ed.; Kluwer Academic Publishers: The Netherlands, 1997; Chapter 28, 387−408.

(2) Grosjean, D. *Sci. Total Environ.* **1991**, *100*, 367−414.

(3) Atkinson, R. Reactions of Oxygen Species in the Atmosphere. In *Active Oxygen in Chemistry*; Valentine, J. S., Foote, C. S., Greenberg, A., Liebman, J. F., Eds.; Blackie Academic and Professional: New York, 1995; Chapter 7.

(4) (a) Knispel, R.; Koch, R.; Siese, M.; Zetzsch, C. *Ber. Bunsen-Ges. Phys. Chem.* **1990**, *94*, 1375−1379. Reported rate constants for the reaction of hydroxycyclohexadienyl with NO_2, NO, and O_2 are the following: $\sim 3 \times 10^{-11}$ cm^3 $molecule^{-1}$ s^{-1}, less than 3×10^{-14} cm^3 $molecule^{-1}$ s^{-1}, and $\sim 2 \times 10^{-16}$ cm^3 $molecule^{-1}$ s^{-1}, respectively. (b) Zetzsch, C.; Koch, R.; Bohn, B.; Knispel, R.; Siese, M.; Witte, F. *Transp. Chem. Transform. Pollut. Troposphere*; Le Bras, G., Ed.; Springer: Berlin, Germany, 1997; Vol. 3, pp 347−256. Approximate atmospheric concentrations of the reactive species can be found for instance in refs 1b, 3, and 13.

10.1021/ja990552l CCC: $18.00
Published on Web 08/31/1999

$[NO_2]$ ratios did not show changes in the yields of the more important products.[5a] This result seems to presuppose that rather similar product yields ensue from either reaction, if they compete. Another illustrative point concerns the formation of $HOO^{\bullet}$.[1,4b,5b] This has been indirectly observed through $OH^{\bullet}$ formation (defined as "prompt") and should, of course, be properly taken into account when postulating oxidation mechanisms. In this respect, one has to heed that it could form in different ways (ref 1a, p 374).

The facts that the steps following the formation of **I** are not well assessed yet[3] and that the field is thus open to speculation justify the undertaking of theoretical investigations. These can provide useful information, complementary to the large amount of experimental results collected so far. Some theoretical studies appeared in the last years. Namely, a 1995 DFT study on toluene[6] was aimed to identify plausible O_2 addition intermediates, on the basis of their relative stabilities (without reaction path study). Then the addition of $OH^{\bullet}$ and O_2 to four methylated hydroxy-cyclohexadienyl radicals was studied in 1996[7] by semiempirical UHF/PM3 geometry optimization of the energy minima (transition structures were located by an approximate procedure), followed by DFT(B3LYP) single-point energy calculations. The thermochemical properties of species involved in photochemical oxidation of benzene were determined in 1996[8a] by the same semiempirical approach, used in conjunction with thermochemical group additivity rules.[8b] Our preliminary theoretical study[9] on the initial steps of the oxidative degradation of benzene (dealing with three different attacks of O_2 on **I**) indicated as viable steps both phenol formation and O_2 addition, which yields the 2-hydroxycyclohexadienyl peroxyl radical intermediate, while benzene oxide formation, recently suggested,[1a] resulted to be much harder.

The oxidation channels of benzene and methylated benzenes can be rather intricate, thus posing some problems also to a theoretical investigation. Benzaldehydes, phenols,[10] 1,2 and 1,4, as well as 1,6 unsaturated dicarbonyls[11,12] are commonly detected products of these degradation processes (ref 1a, pp 374, 375). Incidentally, it can be said that aldehydes are important on their own, because they are involved in aerosol formation, and, through their transformation into peroxyacyl nitrates ($R.CO.OONO_2$), play a role in photochemical smog chemistry.[13] In the case of benzene, the mentioned dicarbonyls are glyoxal, butenedial, and muconaldehyde (hexa-2,4-diene-1,6-dial). The first two could form not only by direct oxidation of the 1,6 dicarbonyl precursor, but also through ring fragmentation channels different from those leading to muconaldehyde. The interest in muconaldehyde itself lies in its toxicity. As its precursor benzene, it exhibits carcinogenic activity (bone marrow toxicity) and has also been shown to be cytotoxic and genotoxic to mammalian cells.[14a] It can be mentioned in this respect that the metabolic pathways from benzene to muconaldehyde and muconic acid have been the subject of several studies, along with the metabolic pathways of muconaldehyde itself, whose chemistry has been investigated recently.[14b]

Because of the complex picture of the possible pathways branching from benzene, the present theoretical investigation is focused on purpose only on part of them. Namely, this paper will deal with those channels that initiate from the intermediate **III**, generated by O_2 addition to **I**, and possibly lead to hexa-2,4-diene-1,6-dial. In analyzing the more likely gas-phase pathways, the two different situations corresponding to high and low NO_x concentrations were considered. Alternative pathways were also explored, of which some were recognized as possibly leading to shorter-chain aldehydes, and left to further investigation.

Method

The study of the reactions discussed below was performed by determining, on the reaction energy hypersurfaces, the critical points corresponding to stable and transition structures. These were fully optimized using gradient procedures[15] at the DFT(B3LYP) level of theory,[16,17] with the polarized split-valence shell 6-31G(d) basis set,[18a] enriched with diffuse sp functions[18b] on the oxygen atoms, hereafter denoted as 6-31(+)G(d). In the figures the more important optimum interatomic distances are reported in ångströms. The nature of the critical points (energy minima, transition structures) was determined by diagonalization of the analytic Hessian (vibrational analysis). The energies relevant to the different reaction pathways were subsequently recomputed at the DFT(B3LYP)/6-311+G(d,p) level,[18c] in correspondence of the DFT(B3LYP)/6-31(+)G(d)-optimized geometries. These DFT doublet energies were corrected for spin contamination by the quartet, by using a formula analogous to that suggested by Yamaguchi.[19] It must be mentioned in this respect that Schlegel and Wittbrodt have recently discussed some drawbacks of the projection procedures, which

(5) Atkinson, R. *J. Phys. Chem. Ref. Data* **1994**, Monograph No. 2, 1−216; *ibid.*, **1989**, Monograph No. 1, 1−246. (b) Siese, M.; Koch, R.; Fittschen, F.; Zetzsch, C. Cycling of OH in the Reaction Systems Toluene/O_2/NO and Acetylene/O_2 and the Addition of OH to Isoprene. In *Transport and Transformation of Pollutants in the Troposphere: Proceedings of the EUROTRAC Symposium '94*; Borrel, P. M., Borrel, P., Cvitas, T., Seiler, W., Eds.; SPB Academic Publishing bv., The Hague: The Netherlands, 1994; pp 115−119.

(6) Bartolotti, L. J.; Edney, O. E. *Chem. Phys. Lett.* **1995**, *245*, 119−122.

(7) Andino, J. M.; Smith, J. N.; Flagan, R. C.; Goddard, W. A., III; Seinfeld, J. H. *J. Phys. Chem.* **1996**, *100*, 10967−10980.

(8) (a) Lay, T. H.; Bozzelli, J. W.; Seinfeld, J. H. *J. Phys. Chem.* **1996**, *100*, 6543−6554. (b) Benson, S. W. *Thermochemical Kinetics*; Wiley-Interscience: New York, 1976.

(9) Ghigo, G.; Tonachini, G. *J. Am. Chem. Soc.* **1998**, *120*, 6753−6757.

(10) Seuwen, R.; Warneck, P. *Int. J. Chem. Kinet.* **1996**, *28*, 315−332.

(11) (a) Dumdei, B. E.; O'Brien R. J. *Nature* **1984**, *311*, 248−250. Yu, J.; Jeffries, H. E.; Sexton, K. G. *Atmos. Environ.* **1997**, *31*, 2261−2280. (b) Yu, J.; Jeffries, H. E. *Atmos. Environ.* **1997**, *31*, 2281−2287.

(12) (a) Klotz, B.; Barnes, I.; Becker, K. H.; Golding, B. T. *J. Chem. Soc., Faraday Trans.* **1997**, *93*, 1507−1516. (b) Shepson, P. B.; Edney, E. O.; Corse, E. W. *J. Phys. Chem.* **1984**, *88*, 4122−4126.

(13) Wayne, R. P. *Chemistry of Atmospheres*; Clarendon Press: Oxford, U.K., 1996; pp 252−263.

(14) (a) Greenberg, A. Exploration of Selected Pathways for Metabolic Oxidative Ring Opening of Benzene Based on Estimates of Molecular Energetics. In *Active Oxygen in Biochemistry*; Valentine, J. S., Foote, C. S., Greenberg, A., Liebman, J. F., Eds.; Blackie Academic and Professional, Chapmann & Hall: New York, 1995; Chapter 8, pp 413−417. (b) Bleasdale, C.; Kennedy, G.; MacGregor, J. O.; Nieschalk, J.; Pearce, K.; Watson, W. P.; Golding, B. T. Chemistry of Muconaldehydes of Possible Relevance to the Toxicology of Benzene. In *Environmental Health Perspectives Supplement, Benzene Toxicity, Carcinogenesis, and Epidemiology*; National Institute of Environmental Health Sciences: Washington, D.C., 1996; Vol. 104, pp 1201−1209.

(15) Pople, J. A.; Gill, P. M. W.; Johnson, B. G. *Chem. Phys. Lett.* **1992**, *199*, 557−560. Schlegel, H. B. In *Computational Theoretical Organic Chemistry*, Csizsmadia, I. G., Daudel, Eds.; Reidel Publ. Co.: Boston, MA, 1981; pp 129−159. Schlegel, H. B. *J. Chem. Phys.* **1982**, *77*, 3676−3681; Schlegel, H. B.; Binkley, J. S.; Pople, J. A. *J. Chem. Phys.* **1984**, *80*, 1976−1981. Schlegel, H. B. *J. Comput. Chem.* **1982**, *3*, 214−218.

(16) Parr, R. G.; Yang, W. *Density Functional Theory of Atoms and Molecules*; Oxford University Press: New York, 1989; Chapter 3. Becke, A. D. *Phys. Rev. A: At., Mol., Opt. Phys.* **1988**, *38*, 3098−3100. Becke, A. D. *ACS Symp. Ser.* **1989**, *394*, 165. Pople, J. A.; Gill, P. M. W.; Johnson, B. G. *Chem. Phys. Lett.* **1992**, *199*, 557−560. Becke, A. D. *J. Chem. Phys.* **1993**, *98*, 5648−5652. Lee, C.; Yang, W.; Parr, R. G. *Phys. Rev. B: Condens. Matter* **1988**, *37*, 785−789.

(17) This theory level was tested on a model reaction and compared with more expensive ab initio methods: Ghigo, G.; Tonachini, G. *J. Chem. Phys.* **1999**, *109*, 7298−7304. It appeared to be a rather good compromise between reliability and feasibility in studying the degradation of aromatics.

(18) (a) Hehre, W. J.; Ditchfield, R.; Pople, J. A. *J. Chem. Phys.* **1972**, *56*, 2257−2261. Hariharan, P. C.; Pople, J. A. *Theor. Chim. Acta* **1973**, *28*, 213−222. (b) Diffuse functions: Clark, T.; Chandrasekhar, J.; Schleyer, P. v. R. *J. Comput. Chem.* **1983**, *4*, 294−301. (c) 6-311+G(d,p): Frisch, M. J.; Pople, J. A.; Binkley, J. S. *J. Chem. Phys.* **1984**, *80*, 3265−3269.

Table 1. Relative Free Energies for the Preliminary Steps in Benzene-OH Oxidation (in Kilocalories per Mole)

benzene-OH + O_2	**I**[a]	0.0
H-abstraction TS **I** − **II**		13.6
phenol + HOO•	**II**	−27.6
addition TS **I** − **III**		15.6
cis peroxyl adduct	**III**	10.5
H-abstraction TS **I** − **IV**		39.5
benzene oxide + HOO•	**IV**	21.0

[a] Bold roman numerals make reference to Scheme 1.

can suggest not to use them.[20] Both projected and unprojected energies are reported in the tables, where only the former are used in conjunction with the above-mentioned vibrational analysis data to provide activation and reaction enthalpies and free energies.[21] All calculations were carried out using the GAUSSIAN94 system of programs.[22,23]

Results and Discussion

1. Preliminary Steps in Benzene-OH Oxidation. Initially, as mentioned above, the reaction of HO• with benzene generates the hydroxy-cyclohexadienyl radical intermediate (**I**). Three alternative ensuing reaction steps were already discussed in the first paper,[9] in which ΔH values were provided. In the following, ΔG estimates computed at 298.15 K will be reported. On one hand, abstraction of the hydrogen *gem* to OH in **I**, operated by O_2, affords phenol (**II**), thus leaving again an aromatic species subject to further oxidation (Scheme 1). For this step, the free-energy barrier is not very high, and the step is quite exoergic (Table 1). On the other hand, O_2 addition to the π-delocalized system of **I** can produce, in a reversible way, the 2-hydroxy-cyclohexadienyl peroxyl radical intermediate (**III**), which opens several possible channels toward further degradation. Although this alternative step is endoergic, the related barrier is just slightly higher than the previous one (Table 1). When these processes are compared with benzene oxide (**IV**) formation, this last pathway does not appear to be competitive, because it is sharply endoergic and is accompanied by a large free-energy barrier (Table 1).

In the following, the Figures 1−4 report the more interesting transition structures relevant to the further evolution of **III**, while Figure 5 summarizes the free-energy changes discussed in this section.

2. O Abstraction by NO in the Peroxyl Intermediate. In polluted areas the concentration of both aromatics and nitrogen oxides is significant (ref 3, p 265). Moreover, the ROO• + NO reaction is generally fast (ref 24, Table 6). Therefore, the first part of this study contemplates the possible intervention of the NO radical (energetics are reported in Table 2). This species reacts with **III** to give, without any energy barrier, a peroxynitrite adduct **V** (Scheme 2), with a large energy drop with respect to the separate reactants, −19 kcal mol^{-1} (the ΔE values reported hereafter are the spin-projected values obtained with the 6-311+G(d,p) basis set). By contrast, the free-energy change results to be much more modest, due to the translational entropy contribution ($\Delta G = -6$ kcal mol^{-1}). Dissociation of **V** to the 2-hydroxy-cyclohexadienyl oxyl radical **VI** and NO_2 requires less than 2 kcal mol^{-1} to exit the energy dip, but in terms of ΔG, there is a further gain of 13 kcal mol^{-1}. If the backward process is considered, no barrier is present on the energy hypersurface to impede reassociation of the fragments **VI** and NO_2 to produce again the peroxinitrite **V**. Thus, **V** corresponds to a depression in both directions (toward **III** or toward **VI**). However, the features of the free-energy surface contrast those of the energy surface (compare the third and fifth columns of Table 2). A more moderate G drop from **III** to **V**, accompanied by a much larger decrease in G from **V** to **VI**, suggests that the importance of the peroxynitrite adduct **V** as an intermediate is rather dubious.

Table 2. Relative Energies for the O-Abstraction by NO (in Kilocalories per Mole)

		ΔE[a]	ΔE[b]	ΔE[c]	ΔH[d]	ΔG[d]
cis peroxyl adduct + NO	**III**[e]	0.0	0.0	0.0	0.0	0.0
peroxynitrite adduct	**V**	−21.1	−19.4	−19.1	−17.5	−6.0
oxyl radical + NO_2	**VI**	−16.8	−16.8	−17.4	−17.6	−19.0

[a] DFT(B3LYP)/6-31(+)G(d) spin-contaminated ΔE values corresponding to optimized geometries. [b] DFT(B3LYP)/6-311+G(d,p) spin-contaminated ΔE values obtained at the DFT(B3LYP)/6-31(+)G(d)-optimized geometries. [c] Spin projected ΔE values. [d] Differential zero-point energy corrections computed at the DFT(B3LYP)/6-31(+)G(d) level. [e] Bold roman numerals make reference to Scheme 2.

Scheme 2

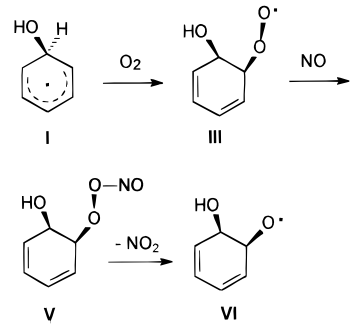

3. Ring Opening to Muconaldehyde. From the hydroxycyclohexadienyl oxyl radical **VI**, β-fragmentation takes place, with a $\Delta G^{\ddagger}$ of 3 kcal mol^{-1}. The relevant transition structure is shown in Figure 1. Arrows in this figure and in the following ones display the major atomic shifts present in the transition vector. The open-chain intermediate **VII** is thus generated (Scheme 3). This step is exoergic by ∼24 kcal mol^{-1} (ΔG). It can be seen in Table 3 that both ΔG values are lower by ∼2 kcal mol^{-1} than the corresponding energy values. One terminus of **VII** is the first carbonyl group of the final dialdehyde, and the second terminus is a planar CHOH center: the unpaired π electron is thus delocalized over the whole system. From **VII**, the second carbonyl group of **VIII** could form by simple H abstraction brought about by O_2. This step requires overcoming a free-

(19) Yamanaka, S.; Kawakami, T.; Nagao K.; Yamaguchi, K. *Chem. Phys. Lett.* **1994**, *231*, 25−33. Yamaguchi, K.; Jensen, F.; Dorigo, A.; Houk, K. N. *Chem. Phys. Lett.* **1988**, *149*, 537−542. See also: Baker, J.; Scheiner, A.; Andzelm, J. *Chem. Phys. Lett.* **1993**, *216*, 380−388.

(20) For discussions concerning the effect of spin projection on the performances of DFT methods, see: Wittbrodt, J. M.; Schlegel, H. B. *J. Chem. Phys.* **1996**, *105*, 6574−6577; Goldstein, E.; Beno, B.; Houk, K. N. *J. Am. Chem. Soc.* **1996**, *118*, 6036−6043.

(21) Reaction enthalpies were computed as outlined, for instance, in: Foresman, J. B.; Frisch, *Æ. Exploring Chemistry with Electronic Structure Methods*; Gaussian, Inc.: Pittsburgh, PA, 1996; pp 166−168. McQuarrie, D. A. *Statistical Thermodynamics*; Harper and Row: New York, 1973; Chapter 8.

(22) GAUSSIAN94: Frisch, M. J.; Trucks, G. W.; Schlegel, H. B.; Gill, P. M. W.; Johnson, B. G.; Robb, M. A.; Cheeseman, J. R.; Keith, T. A.; Petersson, G. A.; Montgomery, J. A.; Raghavachari, K.; Al-Laham, M. A.; Zakrzewski, V. G.; Ortiz, J. W.; Foresman, J. B.; Cioslowski, J.; Stefanov, B. B.; Nanayakkara, A.; Challacombe, M.; Peng, C. Y.; Ayala, P. Y.; Chen, W.; Wong, M. W.; Andres, J. L.; Replogle, E. S.; Gomperts, R.; Martin, R. L.; Fox, D. J.; Binkley, J. S.; Defrees, D. J.; Baker, J.; Stewart, J. P.; Head-Gordon, M.; Gonzalez, C.; Pople, J. A. Gaussian, Inc.: Pittsburgh, PA, 1995.

(23) A typical CPU timing on a DEC Alpha 500/500 station for a single gradient calculation on peroxynitrite **V** was 96 min; the frequency calculation on the same structure took 25 h.

(24) Wallington, T. J.; Dagaut, P.; Kurylo, M. J. *Chem. Rev.* **1992**, *92*, 667−710.

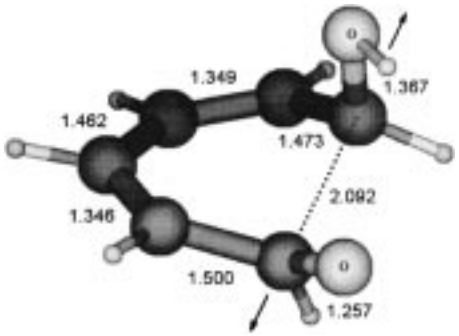

Figure 1. Transition structure for the β-fragmentation taking place in the hydroxycyclohexadienyl oxyl radical **VI**. Bond lengths in ångströms.

Table 3. Relative Energies for the Ring Opening to Muconaldehyde (in Kilocalories per Mole)

		ΔE^a	ΔE^b	ΔE^c	ΔH^d	ΔG^d
oxyl radical	**VI**[e]	0.0	0.0	0.0	0.0	0.0
β-fragmentation TS **VI** − **VII**		6.2	4.5	4.9	3.3	3.0
open-chain radical	**VII**	−17.9	−21.0	−21.4	−22.0	−23.8
open-chain radical + O_2	**VII**	0.0	0.0	0.0	0.0	0.0
H-abstraction TS **VII** − **VIII**		6.8	9.4	7.5	5.4	14.1
muconaldehyde + HOO•	**VIII**	−7.4	−4.9	−3.4	−3.3	−5.2
VII-O_2 adduct	**IX**	−16.8	−13.3	−11.7	−9.2	0.5
HOO• elimination TS **IX** − **VIII**		−8.4	−5.8	−4.3	−5.4	5.0

[a] DFT(B3LYP)/6-31(+)G(d) spin-contaminated ΔE values corresponding to optimized geometries. [b] DFT(B3LYP)/6-311+G(d,p) spin-contaminated ΔE values obtained at the DFT(B3LYP)/6-31(+)G(d)-optimized geometries. [c] Spin projected ΔE values. [d] Differential zero-point energy corrections computed at the DFT(B3LYP)/6-31(+)G(d) level. [e] Bold roman numerals make reference to Scheme 3.

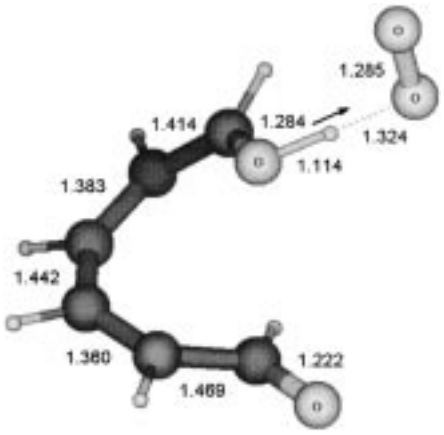

Figure 2. Transition structure for H abstraction operated by O_2 on **VII** to produce **VIII**, muconaldehyde. Bond lengths in ångströms.

energy barrier of ∼14 kcal mol^{-1} (the corresponding energy barrier height is about one-half this value). It would produce muconaldehyde, **VIII**, with a final gain of ∼3 (ΔE) or 5 (ΔG) kcal mol^{-1}. The H abstraction transition structure is displayed in Figure 2. However, an alternative step could see addition of an O_2 molecule on the delocalized radical **VII**. By adding O_2 to the terminal carbon carrying the hydroxyl, we found the step to be exoergic by 12 kcal mol^{-1} in terms of ΔE. By contrast, the ΔG estimate is close to zero. Thus, although the radical coupling takes place without any energy barrier, the G profile would presumably go through a maximum. Then, from the adduct **IX** so obtained, **VIII** can again be produced through a HOO• elimination step. The HOO• concerted elimination transition structure is shown in Figure 3.

The energy barrier for the elimination step is not large, ∼7 kcal mol^{-1}. Its height decreases by ∼3 kcal mol^{-1} in terms of

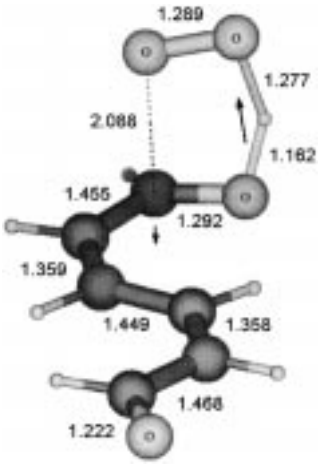

Figure 3. Transition structure for the HOO• elimination step from the adduct **IX**, to give again **VIII**. Bond lengths in ångströms.

Scheme 3

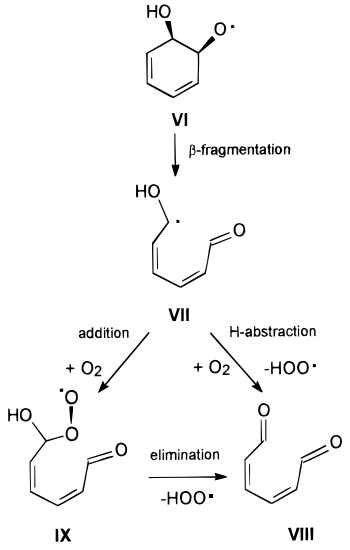

ΔG, putting the **VII**−**IX**−**VIII** process on a better ground with respect to the **VII**−**VIII** H-abstraction step. However, considering the significant amount of energy presumably carried by the system at the end of the energy cascade associated to the preceding transformations, both steps can be regarded as possible.

As recalled in the Introduction, formation of hydroperoxyl has been indirectly detected[1,4,5b] and should be associated to an early step of the degradation mechanism. On the basis of our results, it seems reasonable to relate it to the **I**−**II** step (Scheme 1), and possibly to the free-energy fall of Schemes 2 and 3, where the last step involves HOO• formation. The downhill pathway from **III** is indeed accompanied by an overall free-energy drop of 48 kcal mol^{-1}.

Considering that low NO_x concentration would diminish the importance of this pathway, one has to look for other possibly promising transformations that do not involve nitrogen oxides.

4. H-Abstraction Processes in Peroxyl Intermediates. Two kinds of intramolecular H-abstractions have been examined. The first one is the H-abstraction from the hydroxyl in **III**, operated by the terminal oxygen, which could yield the 2-hydroperoxy-cyclohexadienyl oxyl radical **X** (Scheme 4). This species is similar in some respect to **VI** and could be interesting as a new starting point for ring opening via β-fragmentation. The H transfer could be accompanied (in a concerted or two-step

Scheme 4

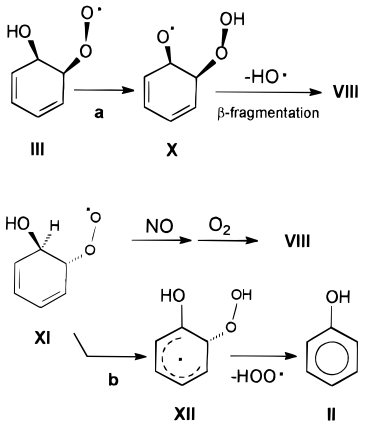

process) by HO• loss, possibly leading to muconaldehyde. The first step, from **III** to **X** (**a** in Scheme 4), sees one hydrogen transferred from the hydroxyl group to the terminal oxygen of the peroxyl group. However, the relevant 6-center TS is associated to a $\Delta G^{\ddagger} = 17$ kcal mol^{-1} with respect to **III**, a value just slightly higher than the step endoergicity. The backward step is therefore easy. For this reason, if the ring-opening pathway shown in Scheme 3 were not viable under a too low NO concentration, the present pathway does not seem to open a likely alternative.

The second intramolecular H-abstraction could take place after **I** has undergone O_2 addition to the π-delocalized system to give **XI** (Scheme 4). This peroxyl adduct is similar to **III** (and has similar stability). It differs from it in that the OO group lies trans with respect to the hydroxyl, while in **III** it is cis. At this point, two pathways could be promising. (i) In the case of high NO_x concentration, a NO-mediated ring opening (via β-fragmentation of **XI**) could take place by a course analogous to that shown for **III** (due to this similarity, it has not been explored in this study). (ii) In **XI** the terminal oxygen of the peroxyl group could as well abstract the hydrogen bound to the carbon *ipso* to the hydroxyl (**b** in Scheme 4). This time the step is very exoergic: the hydroxy-hydroperoxy-cyclohexadienyl radical intermediate product **XII** is more than 19 kcal mol^{-1} below **XI**. This intermediate could, in turn, give phenol by HOO• loss with a further free-energy gain (**II** is 28 kcal mol^{-1} below **I** and 38 kcal mol^{-1} below **III**). However the step from **XI** to **XII** requires overcoming a sizable free-energy barrier: the 5-center TS is estimated 20 kcal mol^{-1} above **XI**. Therefore this process is not competitive with that leading to phenol and studied in ref 6 (step **I**−**II**, $\Delta G^{\ddagger} = 13.6$ kcal mol^{-1}). In conclusion, both intramolecular H-abstractions considered in this subsection are not likely to occur, and it seems reasonable to discard right from the outset the pathways that could originate from them (see Table 4).

5. Ring-Closure Processes of the Peroxyl Intermediate III. Ring closure in **III** by formation of a peroxy bridge could be another promising process. Two ring-closure processes have been considered. Both produce endoperoxidic bicyclic radical intermediates (Scheme 5) and can lead in principle to different fragmentations.

The first ring closure produces a rather stable intermediate **XIII**, whose structure is defined by two fused five- and seven-membered rings, the latter containing a delocalized allyl radical π-system. A similar intermediate (with a methyl group in a central position on the allylic part) was found by Andino et al.[7] This was located at −7.2 kcal mol^{-1} (DFT energy) with respect to the related peroxyl adduct. This is best compared with our unprojected ΔE value of −8.2 kcal mol^{-1} (Table 5, first column). The intermediate **XIII** is 5 kcal mol^{-1} below **III** (ΔG), and the ring-closure TS is associated to a barrier ($\Delta G^{\ddagger}$ =14 kcal mol^{-1} with respect to **III**) which appears to be rather large but not forbidding. This transition structure is displayed in Figure 4. The intermediate **XIII** can thus be expected to open further pathways toward 1,4 and 1,2 dialdehydes (to be dealt with in a forthcoming paper).

The second cyclization mode yields a localized radical **XIV**, whose structure is defined by two fused six-membered rings, one of which contains a double bond, the other the radical center, and the hydroxyl. Its modest stability in terms of ΔG (**XIV** is almost 18 kcal mol^{-1} above **III**) is accompanied by a large energy barrier (the formation TS has a $\Delta G^{\ddagger}$ of more than 24 kcal mol^{-1} with respect to **III**). The above results are in accord with those discussed in refs 6 and 7. Another bicyclic radical, structurally similar to **XIV** and shown in parentheses in Scheme 5, could be obtained by a third cyclization process. Due to the high energy of **XIV**, this pathway was not explored.

Table 4. Relative Energies for the H-Abstraction Processes (in Kilocalories per Mole)

		ΔE^a	ΔE^b	ΔE^c	ΔH^d	ΔG^d
cis Peroxyl adduct	**III**[e]	0.0	0.0	0.0	0.0	0.0
H-abstraction TS **III**−**X**		19.7	19.9	19.9	15.6	16.8
hydroperoxy oxyl radical	**X**	17.4	18.1	18.0	16.8	16.9
trans peroxyl adduct	**XI**	2.0	1.5	1.5	1.6	0.4
H-abstraction TS **XI**−**XII**		25.0	23.6	23.1	20.3	20.7
hydroxy hydroperoxy cyclohexadienyl radical	**XII**	−13.3	−17.0	−17.9	−18.5	−19.1

[a] DFT(B3LYP)/6-31(+)G(d) spin-contaminated ΔE values corresponding to optimized geometries. [b] DFT(B3LYP)/6-311+G(d,p) spin-contaminated ΔE values obtained at the DFT(B3LYP)/6-31(+)G(d)-optimized geometries. [c] Spin projected ΔE values. [d] Differential zero-point energy corrections computed at the DFT(B3LYP)/6-31(+)G(d) level. [e] Bold roman numerals make reference to Scheme 4.

Scheme 5

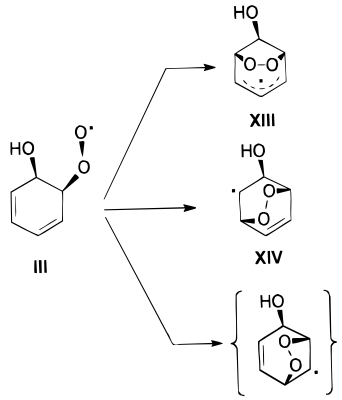

Table 5. Relative Energies for the Ring-Closure Processes (in Kilocalories per Mole)

		ΔE^a	ΔE^b	ΔE^c	ΔH^d	ΔG^d
cis peroxyl adduct	**III**[e]	0.0	0.0	0.0	0.0	0.0
ring-closure TS **III**−**XIII**		13.8	14.6	13.8	12.7	14.2
[3.2.1] peroxyl radical	**XIII**	−8.2	−6.2	−6.8	−6.9	−5.4
ring-closure TS **III**−**XIV**		24.2	25.0	24.6	23.2	24.6
[2.2.2] peroxyl radical	**XIV**	15.4	17.0	17.0	16.5	17.8

[a] DFT(B3LYP)/6-31(+)G(d) spin-contaminated ΔE values corresponding to optimized geometries. [b] DFT(B3LYP)/6-311+G(d,p) spin-contaminated ΔE values obtained at the DFT(B3LYP)/6-31(+)G(d)-optimized geometries. [c] Spin projected ΔE values. [d] Differential zero-point energy corrections computed at the DFT(B3LYP)/6-31(+)G(d) level. [e] Bold roman numerals make reference to Scheme 5.

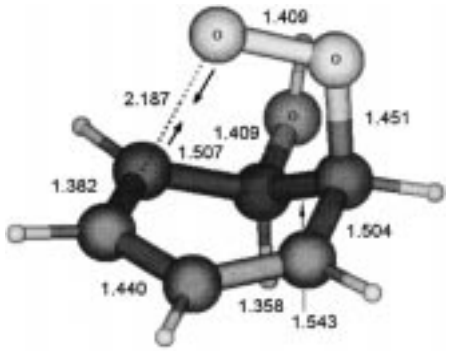

Figure 4. Transition structure for ring closure in **III** to give the bicyclic radical adduct **XIII**. Bond lengths in ångströms.

In Figure 5 a free-energy flow is sketched, only for the three processes that appear to open realistic possibilities on the basis of the theoretical calculations. From the discussion of the preceding subsections, it can be concluded that two are the pathways originating from **III** which can possibly compete: the NO-promoted ring opening of Schemes 2 and 3 (**a** in Figure 5) and the intramolecular process of Scheme 5 leading to **XIII** (**c** in Figure 5). Their relative importance has to be assessed on the basis of the NO concentration. It can be interesting to define the conditions necessary for the two processes to compete with the same rate. However, the step **III** + NO → **V** (Scheme 2) did not allow the detection of a transition structure on the energy hypersurface. For this reason, a computed estimate of $\Delta G^{\ddagger}$ is not immediately available. However, an experimental estimate of the rate constant can be exploited: a value of $k \approx 5 \times 10^9$ M^{-1} s^{-1} was determined for a different system which undergoes the same elementary process (^{i}PrOO$^\bullet$ + NO → ^{i}PrO$^\bullet$ + NO_2).[24] This allows us to attempt drawing a comparison of the second-order reaction of NO and **III** with the first-order ring closure to **XIII**, for which the estimate $k = 2.6 \times 10^2$ s^{-1} results from the computed $\Delta G^{\ddagger}$. It provides the conditions necessary for the two processes to compete with the same rate: the two velocities are equal if [NO] is as high as 5×10^{-8} M, corresponding to 3×10^{13} molecules cm^{-3} (or 1 ppm). On one hand, this tropospheric concentration value can be compared for instance with that reported in ref 13 as typical of a nonpolluted situation: 10^8-10^9 molecules cm^{-3} (or ref 3, pp 254, 255) and results to be very high. On the other hand, a significant NO concentration can be assumed, yet lower than 1 ppm. It can be chosen, for instance, to be lower by an order of magnitude: 0.1 ppm is a value that can be reached in polluted areas (see ref 13, p 252), equivalent to [NO] = 2.7×10^{12} molecules cm^{-3}. The monomolecular and the bimolecular processes will then take place with different rates (υ_1 and υ_2, respectively), whose ratio can be estimated as follows. As $\upsilon_1 = 2.6 \times 10^2$ s^{-1} × [**III**] and $\upsilon_2 = 5 \times 10^9$ $M^{-1}s^{-1}$ × [**III**] × 4.5 10^{-9} M = 22.5 s^{-1}, then $\upsilon_1/\upsilon_2 \approx 11.6$. Therefore, the NO-promoted pathway could be relatively important in polluted areas.

Conclusions

The first step of benzene oxidation is believed to see the formation of the so-called benzene-OH adduct (**I**). Abstraction of the hydrogen *gem* to OH in **I**, operated by O_2 (with $\Delta G^{\ddagger} =$ 13.6), affords phenol, **II**, which can undergo further oxidation. O_2 addition to **I** (with $\Delta G^{\ddagger} = 15.6$ kcal mol^{-1}) can produce (in a reversible way) the 2-hydroxycyclohexadienyl peroxyl radical intermediate, **III**, which opens several possible channels toward further degradation, some of which are considered in this study.

A NO-promoted benzene degradation pathway is described by the present computations as particularly appealing. It leads to ring opening and generation of Z,Z-muconaldehyde. The process is started by O abstraction from the peroxyl group in the 2-hydroxy-cyclohexadienyl peroxyl radical (intermediate **III**) operated by NO. The resulting oxyl radical **VI** is prone to ring opening via β-fragmentation and generates in turn the open-chain radical **VII**. Muconaldehyde can then form either by simple H abstraction operated by O_2 or by O_2 addition followed by hydroperoxyl elimination. The overall sequence is described as a free-energy cascade, with a total gain of 48 kcal mol^{-1}.

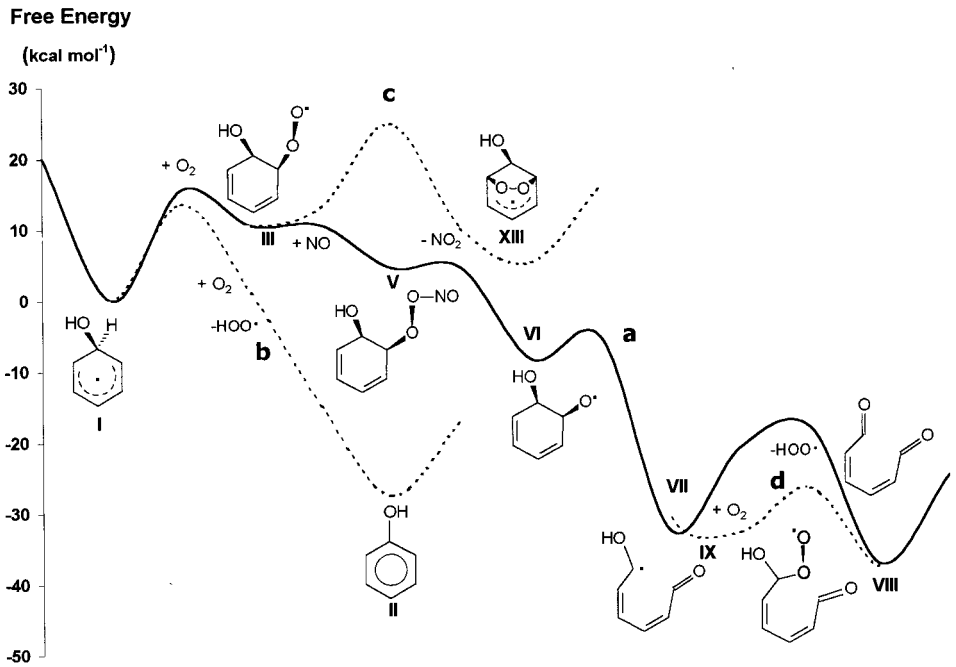

Figure 5. Free-energy flow along different symbolic reaction cooordinates: (a) the NO-promoted ring opening leading to muconaldehyde (solid line); (b) H abstration by O_2, leading to phenol formation (lower dashed line on the left); (c) ring closure of the peroxyl radical to a bicyclic intermediate (upper dashed line on the left); (d) the final formation of muconaldehyde in two different ways (on the right; see text). These are the processes that the theoretical calculations indicate as more promising. Only intermediate structures are displayed.

As an alternative, ring closure to the bicyclic peroxy-bridged intermediate **XIII** seems to be particularly interesting ($\Delta G^{\ddagger} =$ 14.2 kcal mol^{-1} with respect to **III**). This could lead to 1,2 and 1,4 unsaturated aldehydes. Other intramolecular processes have been investigated and do not seem very promising.

An attempt to estimate the relative importance of the NO-promoted and ring-closure pathways (assuming a top NO concentration as reported for polluted areas) has brought to the conclusion that the former can contribute to benzene oxidation up to less than 10% of the latter. In case of low NO_x concentration, the monomolecular process should prevail.

Acknowledgment. Financial support was provided by the Italian MURST.

JA990552L